Quantum path minimization: An efficient method for global optimization

Pu Liu and B. J. Berne
Department of Chemistry and Center for Biomolecular Simulation, Columbia University, New York, New York 10027

(Received 13 August 2002; accepted 17 October 2002)

A new unbiased global optimization approach is proposed, based on quantum staging path integral Monte Carlo sampling and local minimization of individual imaginary time slices. This algorithm uses the quantum tunneling effect to speed up the crossing of energy barriers. This method differs in important ways from previous work on quantum annealing and is able to find all the global minima of Lennard-Jones clusters of size up to $N=100$, except for $N=76$, 77, and 98. The comparison between this new algorithm and several other classes of algorithms is presented.
 [DOI: 10.1063/1.1527919]

I. INTRODUCTION

Global optimization is a crucial and notoriously difficult problem in many fields of science and technology. Many global optimization problems are NP-complete,[1] i.e., a deterministic polynomial time solution is believed not to exist although this has not been proven rigorously. But it has been proven that all NP-complete problems are equivalent, which means that we can get deterministic polynomial-time solutions of other NP-complete problem if we can find one for global optimization. Thus, global optimization is very important from a theoretical perspective.

In testing the efficiency of different methods, many studies have focused on determining the global energy minimum configurations of atomic or molecular clusters. The Lennard-Jones (LJ) cluster is one the most popular test systems. For LJ_{38}, $LJ_{75-77,102-104}$, and LJ_{98}, the location of the global minima is much more difficult since the lowest energy structures of these cases are based, respectively, on the face-centered-cubic (fcc) truncated octahedron, the Marks' decahedra, and the tetrahedron, while the dominant structural motif is the Mackay icosahedron. The global free energy minima and the global potential minima coincide with each other only at very low temperature where the dynamics is very slow. Through great effort over several decades, candidate global energy minima have been found for clusters of size up to $N=150$. Some deterministic approaches, such as the branch and bound method invented by Maranas and Floudas,[2–4] have been applied to LJ clusters; however, its prohibitive computational cost makes this method impractical for large LJ clusters. A wide spectrum of stochastic global optimization routines have been invented and applied to LJ clusters. The biased methods[5–10] make use of the physical insight for particular problems. By constructing appropriate candidates for the energy minimum configuration, and thereby greatly reducing the configuration space to be searched, they can locate almost all the energy minima for clusters of size up to $N=150$. However, it requires substantial knowledge of the system, which is not always available for new systems. Several classes of unbiased methods have been developed, for example the methods based on an annealing algorithm [simulated annealing (SA),[11] quantum annealing,[12,13] multicanonical jumping walk annealing,[14] quantum thermal annealing,[15] and smart walking annealing[16]], various potential deformation methods,[17–23] and some variants of Genetic Algorithms.[24–27]

Delocalization and tunneling in quantum mechanics is the foundation of quantum annealing. Since quantum delocalization softens the potential, it increases the probability of barrier-crossing even at low temperatures. In addition, the zero point energy can be forced to be above all the energy barriers when $\hbar$ is allowed to be sufficiently large. Quantum annealing can be achieved experimentally[28] and theoretically.[12,13,15,29] Through the approximate solution of the Schrödinger equation in an imaginary time[12] or diffusion Monte Carlo,[13] quantum annealing methods have found the correct energy minimum for a series of Lennard-Jones clusters from $n=2$ to 19. Using Quantum Thermal Annealing with PIMC, Lee and Berne found the global minimum of LJ_{38} (Ref. 15) successfully. But for the specific clusters, LJ_{69}, LJ_{75-78}, and LJ_{98}, the task becomes much more difficult.

In this paper, we combine staging path integral Monte Carlo sampling, which efficiently sample barrier crossing events and avoids local trapping, with local minimization,[30] which determines the local energy minimum of Lennard-Jones clusters. Instead of annealing to the classical region ($\hbar \to 0$) and then minimizing to find the global minimum as done in QTA,[15] we do not anneal in $\hbar$, but instead minimize for the configuration of every imaginary time slice. This method appears to be robust and efficient. It locates all the global energy minima of LJ clusters of size up to $N=100$, except for $N=76$, 77, 98. The computational details are described in Sec. II. The comparison with other popular algorithms is presented in Sec. III.

II. METHOD

A. Staging path integral Monte Carlo

Feynman's path integral approach[31] to quantum statistical mechanics allows one to interpret a quantum system as a classical system of ''ring polymers.'' This forms the basis for

path integral Monte Carlo sampling on a classical computer. Under the *primitive* approximation, the primitive partition function[32,33] can be written as

$$Q_P^{\mathrm{prim}}(\beta)=\left(\frac{Pm}{2\pi\beta\hbar^2}\right)^{3NP/2}\int d\mathbf{r_{1,1}}\cdots d\mathbf{r_{i,t}}\cdots d\mathbf{r_{N,P}} \times\exp\left(-\frac{Pm}{2\beta\hbar^2}\sum_{i=1}^{N}\sum_{t=1}^{P}|\mathbf{r_{i,t}}-\mathbf{r_{i,t+1}}|^2 -\frac{\beta}{P}\sum_{\mathbf{t=1}}^{\mathbf{P}}\mathbf{V}(\{\mathbf{r_i}\};\mathbf{t})\right), \tag{1}$$

where P is the trotter number, and N is the number of the particles, $\beta=1/(kT)$, $\mathbf{r_{i,t}}$ is the coordinate of the ith particle in the tth imaginary time slice, and $V(\{\mathbf{r_i}\};t)$ is the system potential of time slice t. This partition function can give a quite accurate description of quantum systems when the trotter number, P, goes to infinity. However, the difference between the true value and this approximate value is usually small when P is large enough. However, the presence of stiff harmonic potentials between the adjacent time slices makes the simulation of quantum systems very inefficient when the trotter number P becomes large. The staging algorithm was proposed to solve this problem.[29,34,35] Instead of moving one bead at a time as done in the primitive algorithm, in the staging algorithm the ''polymer ring'' is divided into several segments and a whole segment is moved at each time step. The staging partition function is

$$Q_P^{\mathrm{stag}}(\beta)=\left[\frac{\beta m\omega_j^2}{2\pi}\prod_{k=2}^{j}\left(\frac{\beta m_k\omega_P^2}{2\pi}\right)\right]^{3Nn/2} \times\int d\mathbf{u_{1,1}}\cdots d\mathbf{u_{i,t}}\cdots d\mathbf{u_{N,P}} \times\exp\left[-\beta\left(\sum_{i=1}^{N}\sum_{s=0}^{n-1}\frac{1}{2}m\omega_j^2|\mathbf{u_{i,sj+1}}-\mathbf{u_{i,(s+1)j+1}}|^2 +\sum_{i=1}^{N}\sum_{s=0}^{n-1}\sum_{k=2}^{j}\frac{1}{2}m_k\omega_p^2\mathbf{u_{i,sj+k}} +\frac{1}{P}\sum_{t=1}^{P}V(\{\mathbf{r_i}(\mathbf{u})\};\mathbf{t})\right)\right], \tag{2}$$

where n and j are the number of ''segments'' and the ''segment length,'' keeping $nj=P$, with $m_k=mk/(k-1)$, $\omega_j=(\beta\hbar)^{-1}\sqrt{P/j}$, $\omega_P=(\beta\hbar)^{-1}\sqrt{P}$. The original Cartesian coordinates, $\mathbf{r_{i,t}}$, can be recursively expressed as the combination of staging coordinates, $\mathbf{u_{i,t}}$,

$$\mathbf{r_{sj+1}}=\mathbf{u_{sj+1}},$$
$$\mathbf{r_{sj+k}}=\mathbf{u_{sj+k}}+\frac{k-1}{k}\mathbf{r_{sj+k+1}}+\frac{1}{k}\mathbf{r_{sj+1}}. \tag{3}$$

From Eq. 2 we can know that the coordinates of the $(j-1)$ beads between fixed end points can be sampled directly from Gaussian distribution. Thus the stiff harmonic force is effectively eliminated. The end points, $\mathbf{r}_{sj+1}$, can be randomly selected to remove the effect caused by the end points being kept fixed.

B. Implementation of quantum path minimization (QPM)

In this paper we introduce and apply the Quantum Path Minimization (QPM) on clusters of atoms interacting according to LJ (12-6) pairwise additive potential,

$$V(\mathbf{r}^N)=4\varepsilon\sum_{i<j}\left(\left(\frac{\sigma}{r_{ij}}\right)^{12}-\left(\frac{\sigma}{r_{ij}}\right)^{6}\right), \tag{4}$$

where r_{ij}, ε, $2^{1/6}\sigma$ are the interatomic distance between the ith and the jth atoms, the pair equilibrium well depth, and distance, respectively.

In order to obtain the global minimum, we sample the effective potential associated with the staging Hamiltonian. We use global MC moves and staging MC moves to update the coordinates. For a global move, all of the P beads representing one particle are randomly displaced within a cube of Δ_{global}, such that the acceptance ratio approaches 0.5 according to the Metropolis criterion. We also move segments of $j-1$ beads in the ''polymer chain'' in staging MC moves. L-BFGS-B,[30] a Fortran subroutine for large-scale bound or unbound contained optimization, is used as the minimization driver.

We noticed that in some of the more difficult LJ clusters, such as LJ_{38} and LJ_{75}, most of the CPU time is spent on unsuccessful random moves around the second-to-lowest energy structure, although this second-to-lowest energy structure is quite easily found. In order to escape from deep local minima, we introduce ''mutations,'' which reset the coordinates of one particle for each time slice randomly in the simulation sphere.

The procedure of QPM is outlined as follows:

(1) Starting from a random configuration of N particles $\{\mathbf{r_i}\}$, choose an appropriate value of $\hbar$, such that the simulation can cross the high-energy barriers frequently. P trotter beads, representing each particle, are then placed overlapping one another on these sites. Define one global move and P staging MC moves of all the particles as one **PIMC** sweep. Conduct n **PIMC** sweeps to let this system expand to some appropriate size. Then the trial configuration for this system becomes $(\{\mathbf{r_{i,1}}\},\ldots,\{\mathbf{r_{i,t}}\},\ldots,\{\mathbf{r_{i,P}}\})$.

(2) For every set of coordinates belonging to some specific imaginary time $t(t=0,\ldots,P)$, we minimize the energy and thus find a minimum. From these minima, we choose the lowest one, $E_{\mathbf{j}}(\{\mathbf{r_j}\})$, where $\{\mathbf{r_j}\}$ represents the coordinates which have the lowest energy E_j. Let $E_j^{\mathrm{old}}=E_j$.

(3) (a) Starting from the trial configuration, $(\{\mathbf{r_{i,1}}\},\ldots,\{\mathbf{r_{i,t}}\},\ldots,\{\mathbf{r_{i,P}}\})$, we run m **PIMC** sweeps and thus get the next trial configuration, $(\{\mathbf{r'_{i,1}}\},\ldots,\{\mathbf{r'_{i,t}}\},\ldots,\{\mathbf{r'_{i,P}}\})$. Then repeat step (2) to get another lowest energy, $E_j^{\mathrm{new}}(\{\mathbf{r'_j}\})=E'_j$.

(b) Compare the two minima: $E_j^{\mathrm{new}}(\{\mathbf{r'_j}\})$ and $E_j^{\mathrm{old}}(\{\mathbf{r_j}\})$.

(c) If $\exp(-\beta(E_j^{\mathrm{new}}-E_j^{\mathrm{old}}))>\zeta$, where ζ is a random number between 0 and 1, let $E_j^{\mathrm{old}}=E_j^{\mathrm{new}}$, and let the coordinates of $\{\mathbf{r'_j}\}$, corresponding to E_j^{new}, to be new

initial classical configuration. After repeating step (1) and step (2), we get another lowest energy $E_j(\{\mathbf{r}_j'\})$ and replace E_j^{new} with E_j. Then go to step (3b).

(d) Otherwise, start with the last trial configuration, $(\{\mathbf{r}_{i,1}\}',\ldots,\{\mathbf{r}_{i,t}\}',\ldots,\{\mathbf{r}_{i,P}\}')$, go to step (3a). Repeat this step at most M times.

(4) If no new minima are found in the last M_1 $(M_1<M)$ steps, generate a mutation by resetting the coordinate of one particle for each time slice by sampling randomly in the simulation box. Go to step (3a).

In our simulation, we introduce the soft wall potential, $V_{\text{wall}}=k_w(r^6-r_0^6)\Theta(r-r_0)$, which defines an effective spherical box to prevent the Lennard-Jones cluster from completely dissociating. The density cannot be taken too high as the particles then hardly move, nor can it be too low. Here, the triple point density of the Lennard-Jones fluid was aimed for. We define n PIMC move and one set of minimizations as one pass. The length of a pass, n should be carefully chosen. If this length is too short, the system will always fall into the initial basin since the size of the ''polymer ring'' will not grow large enough to penetrate into another energy basin. If its length is too large, the system will miss basins that may contain the global minimum.

III. RESULTS AND COMPARISON

It is very difficult to compare the relative performance of different global optimization methods systematically since many authors only gave their final result without describing the computational expense, and many authors have applied their methods only to small cluster sizes or to some special cases. Given the exponentially increasing number of local minima as N becomes large, and the small energy differences between these minima, LJ clusters can be used as a benchmark system for the evaluation of different algorithms. LJ clusters ranging in size from $N=10$ to 150 contain the special cases, e.g., LJ_{38}, $LJ_{75-77,102-104}$, LJ_{98}, whose minima are among the most difficult to determine. This is because the lowest energy structures of these specific clusters are based, respectively, on the face-centered-cubic (fcc) truncated octahedron, the Marks' decahedra, and the tetrahedron, while the dominant structural motif is the Mackay icosahedron. Following a suggestion of Wales,[20] it is reasonable to consider the location of the energy minimum of LJ_{38}, $LJ_{75-77,102-104}$, LJ_{98} as the first, second, and third ''hurdles,'' respectively. For those methods where explicit computational expense has not been given, we use success or failure in determining the first, second and third hurdles correctly as the criteria for comparison between methods. In the meantime, we present the relative computational cost of minimizations and Monte Carlo sweeps because we want to compare methods where minimization is applied to methods where minimization is not applied. A comparison of the relative computational expense of the minimizations and the PIMC moves is summarized in Fig. 1. From Fig. 1, we find that the asymptotic behavior of the average computational cost of the minimization is of order N^2, i.e., the same cost as

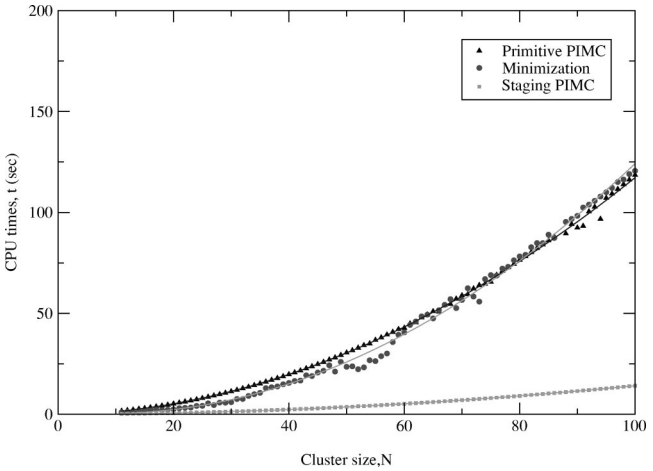

FIG. 1. The computational expense (t) as a function of cluster size N. The time for minimization in this plot is for 40 minimizations, and the time for the PIMC is for 100 sweeps in primitive PIMC and 24 sweeps in staging PIMC with the trotter number $P=40$. The CPU time is for one 450 MHz Pentium II processor. The fitting curve is the result of quadratic regression.

the PIMC sweeps, but it appears that the expense for minimization increases slightly more quickly than that for primitive PIMC sweep when the cluster size is large. We believe that this is because the system will be close to the local minima when we finish the PIMC sweeps, thus the optimizer can locate the local minimum after only a few iterations. The staging path-integral is about eight times as fast as the primitive algorithm in achieving the same ''size'' of the ''polymer ring'' (the special size of the ''polymer ring'' is defined as $(1/NP)\sum_{i=1}^{N}\sum_{t=1}^{P}|\mathbf{r}_{i,t}-\overline{\mathbf{r}_i}|^2$, where $\overline{\mathbf{r}_i}=1/P\sum_{t=1}^{P}\mathbf{r}_{i,t}$), as can be seen from Fig. 1. The typical evolution of the system energy with the time is shown in Fig. 2. To illustrate the performance of our new algorithm, we show the pass number needed to achieve the optimal structure for LJ clusters in the range of 11–55 in Fig. 3. We can locate the global minima

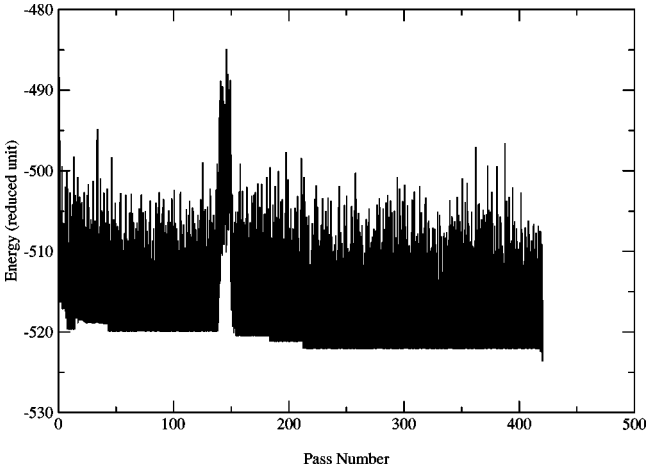

FIG. 2. The total energy vs the pass number for LJ_{95}. The abrupt increase in energy is caused by mutations. We see that the system energy is gradually decreased. When this system is stuck in one local energy minimum, the mutation will jump the system to another point in phase space.

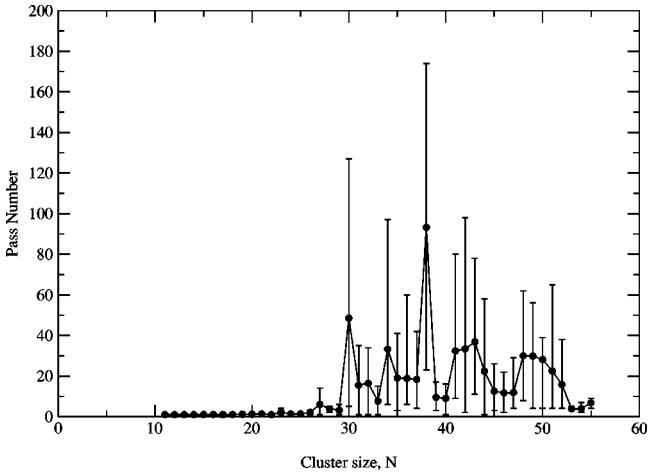

FIG. 3. The pass number needed to locate the global minimum vs the cluster size. For every cluster size, we conduct five independent runs from random configurations. The upper dash and lower dash and the point between them on each vertical bar represent the largest, smallest, and the average value of time steps needed to reach the global minimum.

for LJ_{11-55} in less than 200 passes (consisting of 40 minimizations and 24 staging PIMC sweeps here) with 100% certainty.

A. Comparison with some methods based on annealing

If the annealing rate in simulated annealing is slow enough, finding the global minimum is assured, but this is often not feasible. One shortcoming of the standard simulated annealing approach, and many of its variants arises from the slow relaxation rate at low temperatures. Another shortcoming is that annealing methods spend a large amount of time in the region near local minima. One powerful variant, named multicanonical jump walking annealing (MJWA),[14] couples classical simulated annealing with multicanonical sampling. In MJWA, the canonical Monte Carlo drives the system towards the local minima and the multicanonical sampling surmounts the energy barriers. Unlike its ancestors, this algorithm is quite successfully when applied to LJ_{5-30}. Because LJ_{17} has three low energy structures with very similar geometries and close potential energies ($E_1=-61.318$, $E_2=-61.307$, $E_3=-61.297$), it presents a challenge for global optimization methods. Using the optimized schedule, a total of 4 000 000 MC sweeps is used in each of ten trials. Only one out of ten trials located the exact global minimum for simulated annealing, while the other eight trials got stuck in the second lowest energy minimum. For MJWA, eight out of ten trials found the global minimum, which is eight times better than SA.[14]

We applied our QPM algorithm independently five times to LJ_{17} at the condition of $T=1.0$, $P=40$, $\hbar=1.0$. Our method successfully located the global minimum with 100% assurance within one pass. In each iteration, one pass (40 minimizations and 24 staging PIMC sweeps) was made. That means that the global minimum was determined within a time approximately corresponding to 4500 MC sweeps since the time for one primitive PIMC sweep equals that for P MC sweeps and the time for 40 minimizations approximately equals that for 100 primitive PIMC sweeps. QPM is 880 times more efficient than MJWA and 7000 times more efficient than SA for the global optimization of LJ_{17}.

Another difficult case is the 27-atom Lennard-Jones cluster (LJ_{27}), which has two similar low energy states, with energies $E_1=-112.874$ and $E_2=-112.826$. Even after the length of the simulation is increased to 8 000 000 MC sweeps, only one of ten independent trials located the true global minimum for SA, and five out of ten for MJWA.[14] However, in our algorithm, five out of five independent trials locate the global minimum within 10 passes under the same condition as LJ_{17}, which corresponds to 45 000 MC sweeps. This means our algorithm is 177 times more efficient than MJWA and 885 times more efficient than SA for the cluster LJ_{27}. Comparison between the MJWA, SA, and QPM is summarized in Table I.

B. Comparison with quantum global optimization

Through an approximate solution of the Schrödinger equation in imaginary time[12,36] or diffusion Monte Carlo,[13] some algorithms can find the correct global energy minima for some Lennard-Jones clusters.[12,13] However, some of these methods[36] do not do well even for very small size, i.e., $N=8$ or 9. And those algorithms have been applied only to a series of small clusters LJ_{2-19}.

Lee and Berne[15,29] combined the path integral Monte Carlo method with quantum and thermal annealing (QTA) and applied this method successfully to the BLN protein model. They also successfully found the global minimum of the first hard case LJ_{38}. But their method does not find the global energy minima for the larger ''hard cases.''

Using our algorithm, almost all of the lowest-energy structures of LJ clusters with a size of up to $N=100$ have been located. The first hurdle, LJ_{38}, is easily passed; we can locate the energy minimum in less than 200 passes with

TABLE I. Comparison between the MJWA, SA, and our quantum path minimization. The number of total MC sweeps were employed is same for MJWA and SA, but much less for QPM (the total cost for QPM is expressed in the form of MC sweeps). The successful trials are those that located the global energy minima.

Molecular system	Global minimum	Total MC sweeps		Successful trials/total trials		
		MJWA/SA[a]	QPM	MJWA[a]	SA[a]	QPM
LJ_{17}	−61.318	4×10^6	4.5×10^3	8/10	1/10	5/5
LJ_{27}	−112.874	8×10^6	4.5×10^4	5/10	1/10	5/5

[a]Reference 14.

100% success ratio. We even find the global minimum of one of the second hurdle cluster, LJ_{75}. In QTA, the time-consuming annealing process is repeated again and again and does not stop until the ''polymer ring'' has collapsed into one classical bead even when most beads of the ''polymer ring'' have fallen into the superbasin containing the global minimum. In our algorithm (QPM), we can find the energy minimum even when only *one bead is trapped* near this minimum. To our knowledge, QPM is the most successful of the quantum global optimization algorithms.

C. Comparison with the genetic algorithm (GA)

It is of interest to compare the QPM to genetic algorithms, another widely-used approach for global optimization. The genetic operations such as mating and mutation can generate children which are dramatically different from their parents, such that crossing the energy barriers is not rate-determining. Thus one advantage of the GA is that the system will never be stuck in some local minimum if the selection standard is appropriate. In our algorithm, the path-integral simulation increases the possibility of barrier crossing through quantum tunneling effects. In addition, we adopt a ''mutational'' approach by resetting the coordinates of some beads randomly in the simulation sphere, which partly helps the system escape from the local minimum.

Deaven *et al.*[24] studied the LJ clusters using genetic algorithm. In this paper, the relaxed energies is used as the criteria of fitness. The first hurdle, LJ_{38}, was passed by this modified genetic algorithm. However, the minima for LJ_{69}, LJ_{75-78}, LJ_{98} were missed. Using QPM, we not only found all the minima reported by Deaven, but we also located the minima for LJ_{69} and $LJ_{75,78}$. However, we did not locate the global minima for LJ_{76-77}.

By incorporating new mutational operations (twinning and add-and-etch process), seeding of the initial parent population with some structural motifs frequently encountered in addition to random configurations, and incorporating certain acceleration techniques, the improved genetic algorithm[26] can pass the first and second hurdles. But the introduction of the seeding means that this method is no longer an unbiased one.

In order to compare the relative performance of GA and QPM quantitatively, we ran our program for five runs for each cluster from $N=11$ to $N=55$, since Niesse[27] has reported the best performance of their modified genetic algorithm for cluster from $N=4$ to $N=55$. The CPU times required for our algorithm are given in Fig. 4. From Fig. 1 in Ref. 27, it can be seen that the computational expense for the GA will increase so rapidly when no seed is used that only the global minima for clusters up to $N=29$ were calculated. However, with QPM, the global minima for large clusters can be found in reasonable time even if we start from a random configuration without seeding.

It is important to determine the time scale required for QPM as a function of cluster size. Assuming that the CPU-time can be expressed in the form of the power law, $t \propto N^{\gamma}$ (N is the cluster size), we determined that $\gamma=3.2$ from the $\log(t)$ vs $\log(N)$ data in Fig. 4. The comparison of QPM with DS-GA and SF-GA is given in Table II. From this table we find that our algorithm scales as $O(N^{3.2})$, which means that our algorithm is more efficient than the seeded version of both of these two genetic algorithms as well as the unseeded version at least for the range of clusters used in our study. The seeded genetic algorithm, requires much prior knowledge about the structures of the clusters. Another weakness of the seeded version of the GA is that it is not suitable for the ''hard'' cluster systems, since the genetic information inherited from the cluster of another size will not be helpful in locating the global minimum, but might, in fact, be detrimental to the task by trapping the system in the local minima.

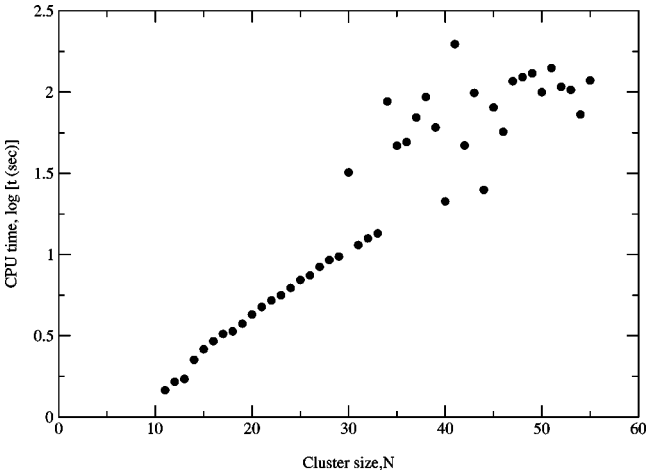

FIG. 4. The logarithm of the CPU time t as a function of cluster size N. Each time shown in the graph is the best result of five independent runs. Note that the Y-axis scale is logarithmic. The CPU time is for one 450 MHz Pentium II processor. The time to calculate the displacement cubes Δ_{global} and Δ_{local} is not included.

D. Comparison with hypersurface transformations

One of the difficulties encountered in the global optimization problem is that the number of local minima grows exponentially with the size of the cluster. Hypersurface deformation-based algorithms[17,18] were designed to surmount this multiple-minima problem. Through deformations of the original potential energy surface (PES), the number of minima can be reduced by orders of magnitude. Thus the topological details of the deformed PES become feasible for us to explore. Using the reversing procedure the original potential is gradually rebuilt. However, the global minimum of the highly deformed PES does not necessarily track back to

TABLE II. Best fit parameters γ of data in Fig. 4. The value of γ is obtained through linear regression of $\log(t)$ vs $\log(N)$. The integers in the brackets represent the fitting bounds of cluster size. For seeded deterministic/stochastic genetic algorithm (DS-GA) and space-fixed genetic algorithm (SF-GA) algorithms, we choose the value of cumulative CPU time as defined in Ref. 27.

	DS-GA[a]	SF-GA[a]	This work
Unseeded	3.9[4–20]	4.4[4–29]	2.0[11–29]
Unseeded	···	···	3.2[11–55]
Seeded	4.5[4–29]	3.3[4–55]	···

[a]Reference 27.

that of the original PES when the highly deformed PES is mapped back to the undeformed PES. In the worst circumstances, the information about the true global energy minimum will be totally washed away when the deformation is conducted, and there is then only a remote possibility to locate it. Some hypersurface deformation methods have passed the first hurdle, LJ_{38}. One of the most sophisticated methods, called self-consistent basin-to-deformed-basin mapping (SCBDBM),[18] locates all the lowest energy structures of the Lennard-Jones atomic clusters up to $N=100$ except for the clusters LJ_{75-77} and LJ_{98}. However, it found the second-to-lowest energy structure for these ''hard cases.'' In this method they couple the superbasins in the original PES to basins in the highly deformed PES iteratively and then try to locate a group of basins including the true energy minimum in the original PES. The distance scaling method (DSM) is used as the deformation scheme and a short Monte Carlo minimization search in the near region of the minima in the original PES is integrated to improve the performance. However, this method is very expensive for large size Lennard-Jones clusters because of the large number of local minimizations in the local search. For example the location of the global minimum of LJ_{70} required 3.5 h using 10 processors on the IBM SP2 supercomputer. In our algorithm, minimization is also used frequently. But the time for each local minimization scales only as N^2 after the PIMC sweeps and the number of such operations is less than in SCBDBM due to the quantum tunneling effect. For LJ_{70}, we can find the minimum in 150 passes with a successful ratio of 4/5, equivalent to only 2.8 h on a single 450 MHz Pentium II processor.

Basin-hopping is one of the most successful algorithms which can efficiently locate the minimum energy of LJ clusters. The transformed energy, $\tilde{E}(\mathbf{X})=\min(\mathbf{E}(\mathbf{X}))$, becomes the energy obtained by minimization from the current configuration. Through the elimination of the transition state and the acceleration effect of the catchment basin transition, all the global energy minima for clusters up to LJ_{110} have been located. The variant of basin-hopping in favor of the downhill moves locates the global minimum of LJ_{98} for the first time.[21] Although the minimum for LJ_{76} was only found in the short runs seeded from the LJ_{75} or LJ_{77} according to the literature,[20] recent unpublished work shows that all the minima can be located without any prior knowledge.[37] In our program, we can locate the minimum of LJ_{75}. The outstanding performance of optimized basin-hopping has been reviewed.[38] For example, it can locate the global minimum of LJ_{70} within 3 min on one 250 MHz Sun Ultra II processor.

Many changes can be implemented to improve the performance of the QPM. For example, it is not necessary to minimize the configuration of every time-slice in the ''polymer rings'' since the configurations of two neighboring time slices are similar. We can optimize the parameters: P (the trotter number), T (simulation temperature), $\hbar$ (the parameter to control the extent of quantization). Since a large amount of local minimizations are used to compare the local minima and the speed of the minimization subroutines are highly dependent on specified tolerances (the stop criterion), we can use a rough tolerance for rough comparison when rejecting the high energy structures and then increase the precision.

IV. CONCLUSIONS

We have introduced the quantum path minimization (QPM) algorithm and applied it to the problem of determining global energy minima for Lennard-Jones clusters containing up to 100 atoms. Using local minimization to locate the local energy minima and staging path-integral Monte Carlo to accelerate the crossing of energy barriers, all the known global minima can be reproduced except for $LJ_{76,77}$ and LJ_{98}. In these cases, our algorithm found the second-to-lowest energy structures instead. The CPU time required to locate the lowest energy structure scales as $O(N^{3.2})$ in the region of $N=11-55$.

Considering the computational expense and the ability to locate the global minima of some special cluster sizes, i.e., the ''hard'' clusters, we have compared the performance of QPM with other popular algorithms. From these comparisons, we have demonstrated the robustness and the efficiency of our new algorithm. We are applying our method to other systems, i.e., Morse clusters, which will provide a critical test.

ACKNOWLEDGMENTS

One of the authors, P. L. thanks Dr. Huafeng Xu, Dr. Claudio Margulis, Dr. Goran Krilov, and Dr. Y. Lee for stimulating discussions and kind help in programming from Dr. Harry Stern. This work has been supported by a grant for B.J. B. from the NIH (GM4330).

[1] M. Gary and D. Johnson, *Computers and Intractability: A Guide to the Theory of NP-Completeness* (Freeman, San Francisco, 1979).
[2] C. Maranas and C. Floudas, J. Chem. Phys. **97**, 7667 (1992).
[3] C. Maranas and C. Floudas, J. Chem. Phys. **100**, 1247 (1994).
[4] D. Standley, V. Eyrich, A. Felts, R. Friesner, and A. McDermott, J. Mol. Biol. **285**, 1691 (1999).
[5] M. R. Hoare and P. Pal, Adv. Phys. **20**, 161 (1971).
[6] J. P. K. Doye, D. J. Wales, and R. S. Berry, J. Chem. Phys. **103**, 4234 (1995).
[7] J. P. K. Doye and D. J. Wales, Chem. Phys. Lett. **247**, 339 (1995).
[8] J. A. Northby, J. Chem. Phys. **87**, 6166 (1987).
[9] T. Coleman and D. Shalloway, J. Global Optim. **4**, 171 (1994).
[10] G. L. Xue, J. Global Optim. **4**, 425 (1994).
[11] S. Kirkpatrick, C. Gelatt, and M. Vecchi, Science **220**, 671 (1983).
[12] P. Amara, D. Hsu, and J. Straub, J. Phys. Chem. **97**, 6715 (1993).
[13] A. Finnila, M. Gomez, C. Sebenik, C. Stenson, and J. Doll, Chem. Phys. Lett. **219**, 343 (1994).
[14] Huafeng Xu and B. J. Berne, J. Chem. Phys. **112**, 2701 (2000).
[15] Y. Lee and B. Berne, J. Phys. Chem. A **104**, 86 (2000).
[16] Ruhong Zhou and B. J. Berne, J. Chem. Phys. **107**, 9185 (1997).
[17] J. Pillardy and L. Piela, J. Phys. Chem. **99**, 11805 (1995).
[18] J. Pillardy, A. Liwo, and H. A. Scheraga, J. Phys. Chem. A **103**, 9370 (1999).
[19] Zhongwei Zhu, M. E. Tuckerman, Shane O. Samuelson, and Glenn J. Martyna, Phys. Rev. Lett. **88**, 100201 (2002).
[20] D. J. Wales and J. P. K. Doye, J. Phys. Chem. A **101**, 5111 (1997).
[21] H. Leary and J. P. K. Doye, Phys. Rev. E **60**, 6320 (1999).
[22] W. Wenzel and K. Hamacher, Phys. Rev. Lett. **82**, 3003 (1999).
[23] C. Barron, S. Gomez, and D. Romero, Appl. Math. Lett. **9**, 75 (1996).
[24] D. M. Deaven, N. Tit, J. R. Morris, and K. M. Ho, Chem. Phys. Lett. **256**, 195 (1996).
[25] S. K. Gregurick, M. H. Alexander, and B. Hartke, J. Chem. Phys. **104**, 2684 (1996).

[26] M. D. Wolf and U. Landman, J. Phys. Chem. A **102**, 6129 (1998).
[27] J. A. Niesse and Howard R. Mayn, J. Chem. Phys. **105**, 4700 (1996).
[28] J. Brooke, D. Bitko, T. F. Rosenbaum, and G. Aeppli, Science **284**, 779 (1999).
[29] Yong-Han Lee and B. J. Berne, J. Phys. Chem. A **105**, 459 (2001).
[30] C. Zhu, R. H. Byrd, P. Lu, and J. Nocedal, Northwestern University EECS Technical Report NAM12 (1995).
[31] R. P. Feynman and A. R. Hibbs, Quantum Mechanics and Path Integrals (McGraw–Hill, New York, 1965).
[32] H. F. Jordon and L. D. Fosdick, Phys. Rev. **171**, 128 (1968).
[33] J. A. Barker, J. Chem. Phys. **70**, 2914 (1979).
[34] M. E. Tuckerman, B. J. Berne, G. J. Martyna, and M. L. Klein, J. Chem. Phys. **99**, 2796 (1993).
[35] E. L. Pollock and D. M. Ceperley, Phys. Rev. B **30**, 2555 (1984).
[36] J. Kostrowicki, L. Piela, B. J. Cherayil, and H. A. Scheraga, J. Phys. Chem. **95**, 4113 (1991).
[37] D. J. Wales (private communication, 2002).
[38] D. J. Wales and H. A. Scheraga, Science **285**, 1368 (1999).